Interference effects in rotational-state-resolved collisional energy transfer between the A2Π and X2Σ+ states of CN

3 AUTHORS, INCLUDING:

Paul J Dagdigian
Johns Hopkins University
323 PUBLICATIONS **6,145** CITATIONS

INTERFERENCE EFFECTS
IN ROTATIONAL-STATE-RESOLVED COLLISIONAL ENERGY TRANSFER
BETWEEN THE A²Π AND X²Σ⁺ STATES OF CN

Nick FURIO, Ashraf ALI and Paul J. DAGDIGIAN

Department of Chemistry, The Johns Hopkins University, Baltimore, MD 21218, USA

An optical–optical double resonance technique has been used to study transfer between specific quantum levels in the $A^2\Pi$ and $X^2\Sigma^+$ states of the CN radical in collisions with argon. Specific rotational levels within the $v = 7$ A state vibrational level are prepared by laser excitation in the A–X (7,2) band, while collisionally populated levels in this vibrational level and the nearly isoenergetic $v = 11$ level in the X state are probed by laser fluorescence excitation in the interleaved B–A (8,7) and B–X (8,11) bands. The collisional transfer rate from the relatively unperturbed $N = 6$ F_1 Λ-doublets to the X state is comparable to or faster than that for pure A → A inelastic transitions. A significant alternation in the population of even versus odd N levels in the X state is observed, related to the near-homonuclear character of the CN–Ar interaction potentials.

1. Introduction

Collisional quenching of electronically excited molecules has been the subject of numerous experimental studies and continues to evoke great interest. A special class of these experiments includes those involving the $A^2\Pi$ and $X^2\Sigma^+$ states of the isoelectronic CN [1], CO^+ [2,3], and N_2^+ [4,5] molecules, as well as the low-lying triplet states of N_2 [6,7]. In these studies it was possible to monitor the fate of the quenched molecules, in contrast to conventional quenching studies. Collisional interelectronic transfer between the $A^2\Pi$ and $B^2\Sigma^+$ states was also inferred as the origin of anomalous rotational line intensities in early work on CN flames [8,9].

The facile collision-induced transitions between these electronic states were explained [10] as arising from the known non-Born–Oppenheimer mixing [11] between the rovibrational levels of the relevant electronic states in the free molecule. A similar, but more sophisticated, model [12–14] has been utilized to understand collisional transitions among the low-lying electronic states of the alkaline earth oxides. The recent observation [5] of rapid E → E transfer between the $A^2\Pi_u$ and $X^2\Sigma_g^+$ states of N_2^+, as well as among the $A^3\Sigma_u^+$, $B^3\Pi_g$, and $W^3\Delta_u$ states of N_2

[6,7], indicates that perturbations in the isolated molecule are not essential in facilitating these collisional processes. In homonuclear diatomics, the permutation-inversion symmetry prohibits mixing between g and u electronic states in the isolated molecule.

With the exception of the recent experiments by Katayama [5] on N_2^+, E → E transfer has not been studied with rotational and/or fine-structure resolution of the initial and final states. State-resolved experiments [15–21] on pure rotational transfer in open-shell molecules revealed the existence of a propensity for conservation of fine-structure and/or Λ-doublet level, as had been predicted theoretically by Alexander and co-workers [16,22–24]. Recently, Alexander and Corey [25] presented the exact quantum description of collision-induced transitions between quantum levels of $^2\Pi$ and $^2\Sigma$ electronic states.

We have begun a study, with initial and final quantum state resolution, of collisional transfer between the $A^2\Pi$ and $X^2\Sigma^+$ states of the CN radical. We employ an optical–optical double resonance (OODR) technique, as has been utilized in Katayama's study of N_2^+ [5]. Here a pump laser excites a specific initial level, and collisionally populated levels are monitored

through fluorescence excitation by a probe laser. In the heteronuclear CN molecule, the importance of isolated-molecule perturbations can be probed by comparing the collisional behavior of perturbed and unperturbed levels. In addition, the validity of propensity rules inferred from the general theoretical treatment [25] can be tested. Finally, it is possible to determine the relative efficiency of collisional inter-electronic and intra-electronic transfer by comparison of $B\,^2\Sigma^+-X\,^2\Sigma^+$ and $B\,^2\Sigma^+-A\,^2\Pi$ probe laser-induced fluorescence intensities. We note that this was not possible in N_2^+ because the g$\leftrightarrow$u selection rule for radiative transitions prohibited the study of energy transfer within the $A\,^2\Pi_u$ state by the OODR technique.

2. Apparatus

Cyanide radicals were generated in a flow of argon at 1.9 Torr through collisional dissociation of cyanogen (Matheson) by metastable argon atoms produced in a dc discharge [26]. A trace amount of C_2N_2 was added to the flow (approximately 30 mTorr pressure rise). The reaction took place about 10 cm upstream of the optical detection zone to allow the CN radicals to relax radiatively to the ground electronic state.

Grazing-incidence dye lasers [27] (bandwidth ≈ 0.1 cm^{-1}) were employed for both the pump and probe beams and are pumped by the second harmonic of a Nd : YAG laser (Quantel YG581C) and a XeCl excimer laser (Lambda Physik EMG 53 MSC), respectively. The dye laser pulse energies were 25 and 8 mJ, respectively; the energies at the reaction chamber are considerably lower, however. The two beams were overlapped by means of a dichroic mirror and directed into the reaction chamber. The delay between the firing of the Nd : YAG and excimer lasers was controlled electronically, and the time between the 10 ns long light pulses was set with the help of a fast photodiode. For the present experiments, the time between pump and probe pulses was varied between 0 and 20 ns. The laser fluorescence signal was detected through a filter by a photomultiplier (EMI 9816 or 9813 for A–X or B–X detection, respectively) and fed into a boxcar averager, whose output was directed into a chart recorder or laboratory minicomputer. For the OODR scans, a narrow-band filter centered at

390 nm was used to detect B–X emission and block scattered laser light.

3. Results

Specific quantum levels within the $v = 7$ vibrational level of the $A\,^2\Pi$ electronic state of CN were prepared by pump laser excitation of isolated rotational lines in the A–X (7,2) band near 588 nm [28]. This particular vibrational manifold was chosen for initial study because the perturbation due to the $X\,^2\Sigma^+$ electronic state reaches a maximum at an accessible J value (13.5 in the F_1 f manifold [11]), with considerable mixing of the electronic states. (The X state character Σ reaches a maximum of 42.6% [11].) The specific X state vibrational level involved in the perturbation is $v = 11$.

The probe laser interrogated the populations of rotational levels in the $v = 7$ level of the A state, as well as in the nearly isoenergetic $v = 11$ level of the X state, by fluorescence excitation near 492 nm of the B–A (8,7) and B–X (8,11) bands, which are interleaved in each other. A detailed analysis of these bands, along with a comparison of their relative band strengths, will be presented in a future publication. We note that because of the perturbation, it is necessary to known the relative phases of the electronic transition
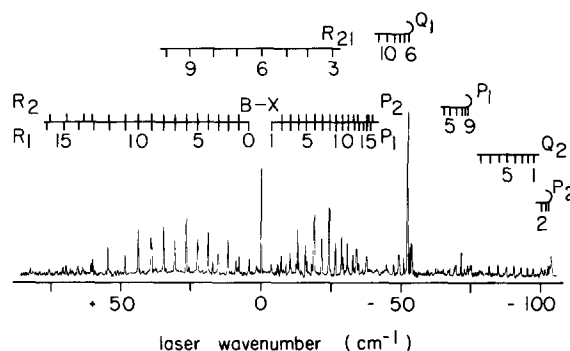

Fig. 1. Probe laser fluorescence excitation spectrum of the CN B–A (8,7) and B–X (8,11) bands near 492 nm with the pump laser tuned to the $Q_1(6)$ line of the A–X (7,2) band. The N'' quantum number is given for individual rotational lines. The R_1 and R_2 branches of the B–A band are omitted since their individual members are weak or overlapped. The very weak R_{12} branch, which occurs to the red of the P_2 head, is also not plotted. The $Q_1(6)$ B–A line is off scale in the plot.

moments for the calculation of rotational line strength factors [16].

Fig. 1 presents a probe laser scan when the $N = 6$ F_1 f level ($J = 6.5$, $\Omega = 3/2$, total parity $-$) is initially excited by irradiation of the pump laser on the $Q_1(6)$ line of the A–X (7,2) band. The strongest lines in the OODR spectrum are the $Q_1(6)$ and $R_{21}(6)$ lines, which probe the laser excited initial level. The delay between the pump and probe lasers was 20 ns for fig. 1. With the lasers coincident in time, the only significant features were the parent lines. At 50 ns delay, the OODR spectrum begins to show evidence of multiple collision effects.

The most striking feature in fig. 1 is the prominence of the B–X rotational lines. To judge by the fluorescence intensities, it appears that collisional A → X transfer is much more probable than pure rotational transfer within the A state. We have calculated the intensity factors for fluorescence excitation in both the B–A and B–X bands. These are found to be approximately a factor of 2 larger for the overlapped $R_{1,2}$ B–X lines than for the Q_1 B–A lines. The relative intensity factors are fairly insensitive to the relative phases of the B–A and B–X transition moments, at least away from the perturbation. In spite of the fact that the B–X electronic transition moment is much larger than that for the B–A transition [29,30], the B–X (8,11) band has a comparable strength to the B–A (8,7) band because of a much smaller Franck–Condon factor [11] for the former. From this calculation, we conclude that the population of the most probable final X state ($N = 6$ or 8) is approximately equal to that for the collisionally populated A state levels adjacent to the initially excited level. Thus, the collisional rate for A → X transfer is comparable to or larger than that for pure A → A inelastic transitions.

We also note a significant alternation in the intensities, and hence populations, of the even versus odd N levels in the collisionally populated X state. When the e parity component is instead initially excited by pumping the $P_1(7)$ line of the A–X band, the odd N levels in the X state are most highly populated. This suggests that this alternation is not an artifact but is related to the symmetries of the initial and final states. In addition, a similar preference for even J changes is evident in rotational transitions within the A state, as seen in particular in the Q_1 branch of the B–A band.

4. Discussion

The observation of facile A → X transfer from relatively unperturbed levels and of the even–odd alternation in the populations of the final levels is very significant for an understanding of the dynamics of collisional interelectronic transfer. The initially excited $N = 6$ F_1 f level is significantly below the most perturbed $N = 13$ level in this manifold and is calculated [11] to possess only 0.2% X state character; the F_1 e level is even less perturbed (Σ equals 0.1%). The present results on CN, along with Katayama's observations on N_2^+ [5], show that, at least in these molecules, it is not necessary to funnel through highly perturbed levels in order to undergo collisional transitions to another, nearly isoenergetic electronic state.

The alternation in final state populations is related to the near homonuclear nature of the CN charge distribution. In a true homonuclear molecule, collisional transitions within and between $^2\Pi$ and $^2\Sigma^+$ states are strictly forbidden between s and a nuclear permutation levels, as shown theoretically by Alexander and Corey [25] and seen experimentally by Katayama [5] in N_2^+. The initial $N = 6$ F_1 f level would be s with respect to nuclear interchange in $D_{\infty h}$ molecular symmetry if the A state were ungerade [25], as in the isoelectronic N_2^+ molecule; likewise the $N = 6$ F_1 e level would have a symmetry. Within the $^2\Sigma_g^+$ state, both spin doublets of even and odd N levels have s and a symmetry, respectively. Thus, the enhancement of the observed transfer rate into the even and odd N X state manifolds in the case of initial population of the $N = 6$ F_1 f and F_1 e initial levels, respectively, is consistent with a residual conservation of nuclear permutation symmetry. A similar alternation has been observed in rotationally inelastic scattering experiments involving NO(X $^2\Pi$)–Ar collisions [18] and in semiclassical model calculations [31]. This alternation in final populations was ascribed to the fact that the interaction energy depended only weakly on which end of the molecule faced the atomic perturber.

Alexander and Corey [25] have shown that transitions within and between $^2\Pi$ and $^2\Sigma^+$ states induced by a structureless target are governed by four different electronic surfaces in a diabatic description. Three of these refer to the atom–molecule electrostatic potential energy surfaces when the electronic wavefunc-

tion of the molecule is Σ, $\Pi(A')$, and $\Pi(A'')$; A' and A'' designate the reflection symmetry with respect to the triatomic plane. The fourth surface, denoted V_1 by Alexander and Corey [25], represents the off-diagonal electrostatic matrix element between the Σ and $\Pi(A')$ wavefunctions, which are mixed by the approach of the perturber.

In the IOS approximation, the $\Pi \rightarrow \Sigma$ inelastic cross sections can be written as [25]

$$\sigma(^2\Pi\, J\Omega e \rightarrow\, ^2\Sigma\, J'e')$$

$$\sum_{l \geqslant 1} \tfrac{1}{2}[1 - \epsilon\epsilon'(-1)^{J+J+l}](2J'+1)$$

$$\times \left[\begin{pmatrix} J' & l & J \\ -1/2 & 1 & -1/2 \end{pmatrix}^2 \delta_{\Omega,1/2} \right.$$

$$\left. + \begin{pmatrix} J' & l & J \\ -1/2 & -1 & 3/2 \end{pmatrix}^2 \delta_{\Omega,3/2} \right] \sigma_l^1, \qquad (1)$$

where ϵ and ϵ' are the symmetry indices [25] of the initial and final states. Case (a) coupling has also been assumed in eq. (1). The base cross sections σ_l^1 can be obtained from a fixed-angle scattering calculation involving the diagonal Σ and $\Pi(A')$ potentials, as well as the off-diagonal V_1 potential.

In the case of a homonuclear molecule, the even l terms vanish for coupling between Σ_g^+ and Π_u states. (These are the symmetry designations for the corresponding states of the isoelectronic N_2^+ molecule.) Model calculations [32] indicate that the final state alternations observed here are consistent with the assumption that the "homonuclear forbidden" even l base cross sections are reduced by 50% with respect to the "homonuclear allowed" odd l terms. The observation of a residual homonuclear character is supported by a nearly symmetric charge distribution: The dipole moment in the CN A state is calculated to be only 0.05 D [33].

We are in the process of taking OODR spectra for a range of initial $v = 7$ A state levels in order to determine state-to-state inelastic rate constants. We hope to compare these results with a fully quantum mechanical analysis planned by Alexander [33] in order to understand in more detail the mechanism of interelectronic energy transfer in CN.

Acknowledgement

References

[1] D.H. Katayama, T.A. Miller and V.E. Bondybey, J. Chem. Phys. 71 (1979) 1662.

[2] V.E. Bondebey and T.A. Miller, J. Chem. Phys. 69 (1978) 3597.

[3] D.H. Katayama and J.A. Welsh, J. Chem. Phys. 79 (1983) 3627; Chem. Phys. Letters 106 (1984) 74.

[4] D.H. Katayama, T.A. Miller and V.E. Bondybey, J. Chem. Phys. 72 (1980) 5469.

[5] D.H. Katayama, J. Chem. Phys. 81 (1984) 3495; Phys. Rev. Letters 54 (1985) 657.

[6] N. Sadeghi and D.W. Setser, Chem. Phys. Letters 77 (1981) 308; 82 (1981) 44; J. Chem. Phys. 79 (1983) 2710.

[7] A. Rotem, I. Nadler and S. Rosenwaks, Chem. Phys. Letters 83 (1981) 281; J. Chem. Phys. 76 (1982) 2109.

[8] H.E. Radford and H.P. Broida, J. Chem. Phys. 38 (1963) 644.

[9] D.W. Pratt and H.P. Broida, J. Chem. Phys. 50 (1969) 2181.

[10] W.M. Gelbart and K.F. Freed, Chem. Phys. Letters 18 (1983) 470.

[11] A.J. Kotlar, R.W. Field, J.I. Steinfeld and J.A. Coxon, J. Mol. Spectry. 80 (1980) 82.

[12] M.H. Alexander, J. Chem. Phys. 76 (1982) 429.

[13] M.H. Alexander and M. Osmolovsky, J. Chem. Phys. 77 (1982) 839.

[14] B. Pouilly, J.-M. Robbe and M.H. Alexander, J. Phys. Chem. 88 (1984) 140.

[15] P.J. Dagdigian and S.J. Bullman, J. Chem. Phys. 82 (1985) 1341.

[16] M.H. Alexander, S.L. Davis and P.J. Dagdigian, J. Chem. Phys. 83 (1985) 556.

[17] R.K. Lengel and D.R. Crosley, J. Chem. Phys. 67 (1977) 2085.

[18] P. Andresen, H. Joswig, H. Pauly and R. Schinke, J. Chem. Phys. 77 (1982) 2204.

[19] P. Andresen, D. Häuseler and H.W. Lülf, J. Chem. Phys. 81 (1984) 571.

[20] O. Nedelec and J. Dufayard, Chem. Phys. 84 (1984) 167.

[21] C. Dufour, B. Pinchemel, M. Douay, J. Schamps and M.H. Alexander, Chem. Phys. 98 (1985) 315.

[22] M.H. Alexander, J. Chem. Phys. 76 (1982) 3637, 5974.

[23] M.H. Alexander and S.L. Davis, J. Chem. Phys. 79 (1983) 227.

[24] M.H. Alexander and B. Pouilly, J. Chem. Phys. 79 (1983) 1545.

[25] M.H. Alexander and G.C. Corey, J. Chem. Phys. 84 (1986) 100.

[26] T. Urisu and K. Kuchitsu, J. Photochem. 2 (1973/74) 409.

[27] M.G. Littman and H.J. Metcalf, Appl. Optics 17 (1978) 2224.

[28] S.P. Davis and J.G. Phillips, The red system of CN (University of California Press, Berkeley, 1963).

[29] J.B. Halpern and X. Tang, Chem. Phys. Letters 97 (1983) 170.

[30] M. Costes, C. Naulin and G. Dorthe, Chem. Phys. Letters 113 (1985) 569.

[31] C.W. McCurdy and W.H. Miller, J. Chem. Phys. 67 (1977) 463.

[32] M.H. Alexander, unpublished.

[33] H.-J. Werner, P.J. Hay and D.C. Cartwright, J. Chem. Phys., submitted for publication.